Electronic Supplementary Material (ESI) for Nanoscale.

Supporting Information of "Exhaustive classification and systematic free-energy profile study of single-stranded DNA inter-overhang migration"

Hon Lin, Too[1,2] and Zhisong, Wang[1,2,*]

[1]NUS Graduate School for Integrative Science and Engineering, National University of Singapore, Singapore 117542

[2]Department of Physics, National University of Singapore, 2 Science Drive 3, Singapore 117542

[*]Email: phywangz@nus.edu.sg

Contents

1 Iterative reweighing umbrella sampling method

To ensure the data are well-sampled, we employed the iterative reweighing method described below:

1. Run the first Virtual Move Monte Carlo(VMMC) with a pre-determined weight file for 10^7 simulation steps. Ensure each state is visited at least once.
2. Add the new data to the previously collected data. Calculate the relative free energy from the unbiased frequency.
3. Generate a histogram of the biased frequency.
   (a) If the histogram is almost flat, the collected data has achieved statistical significance
   (b) If the histogram is heavily skewed, regenerate a new weight file based on the accumulated free energy profile. Run a new independent simulation and repeat Step 2-3.
4. After collecting enough data, the relative free energy profile with respect to the reference state is obtained from the following formula

$$\frac{\Delta G(x)}{k_B T} = -\ln\left(\frac{N(x)}{N_r}\right) \tag{1}$$

   where $N(x)$ is the unbiased frequency of state x, and N_r is the unbiased frequency of the reference state r. We chose $r = 1.7$nm as the contact window's reference state, and the most frequently visited state as the displacement window's reference state. SFigure 1 shows how the iterative reweighing method improves the statistic of hopping migrator on a 10bp track.

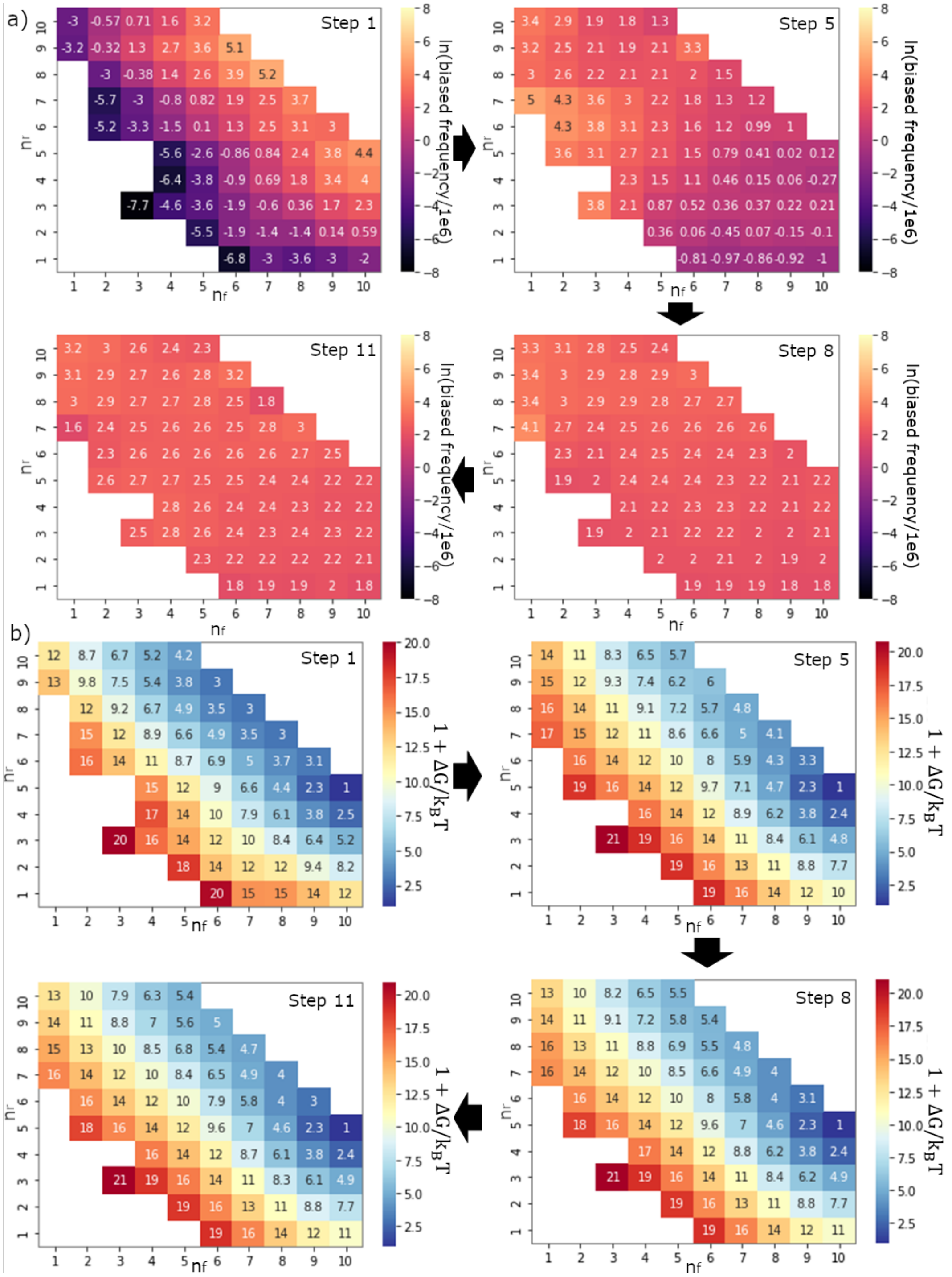

SFigure 1: The iterative reweighing method as applied to the hopping migrator on a 10bp track in the displacement window. Panel a and panel b show the change in biased frequency and relative free energy, respectively, in step 1, 5, 8 and 11.

2 Migrator-track sequence

2.1 15nt migrator sequence

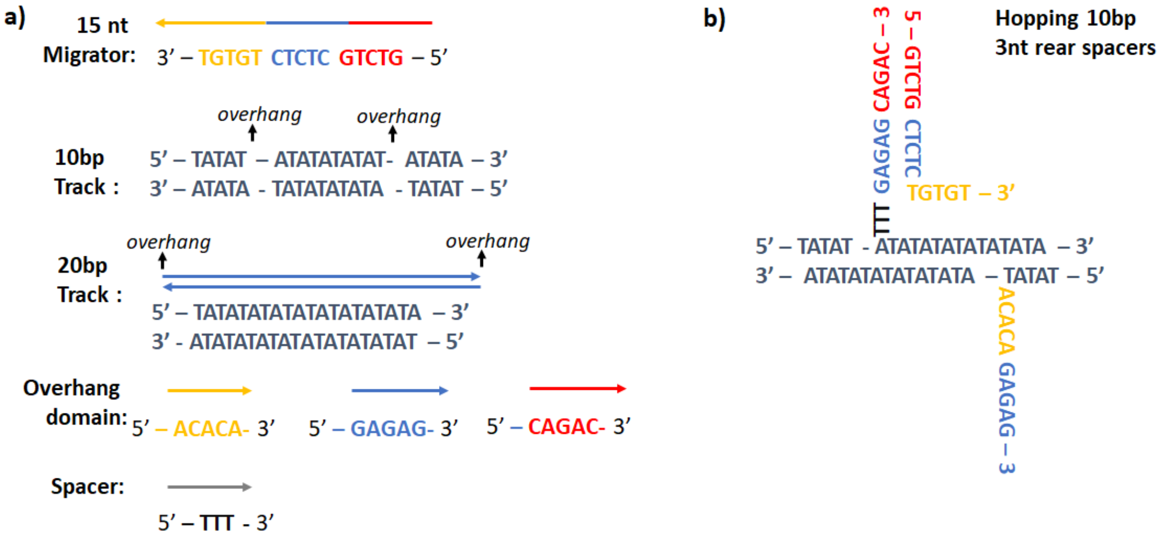

SFigure 2: The nucleotide sequence of a 15nt long migrator. **(a)** shows the sequence of each color-coded domain. The nucleotide sequence is the same for all migration gaits, the difference lies in the position of overhang domain as depicted in Figure 1c. The overhang domain can be seen as the lego piece to obtain the required gait. We provide an example in **(b)**, which shows the sequencing of a hopping gait on a 10bp 3nt rear spacers track.

2.2 18nt cartwheeler sequence

SFigure 3: The nucleotide sequence of a 18nt cartwheeling migrator on a 20bp track with 3nt spacers at both the front and rear footholds.

3 Minimum Path Sum

Given a $m \times n$ matrix with non-negative number, with a starting state of (0,0), and a final state of (m-1,n-1), the minimum path sum (or the minimum cost path) is the path that minimizes the sum of all numbers that it passes through.

Here, the 2D free energy landscape is transformed into a $n_r \times n_f$ matrix. We shift the relative free energy upward by $1k_BT$ to ensure the relative free energy is always larger or equal to $1k_BT$. From causality, we demand the pathway to strictly take vertical or horizontal cell transition only (no diagonal transition is allowed). The starting state is $(n_f, n_r) = (1, 10)$ and the final state is $(10, 1)$ on the isoenergetic track or $(14, 1)$ on the downhill track. The total free energy for each possible pathway is calculated by adding up all the visited path's relative free energy, and the path with the lowest total free energy is the minimum path sum.

4 Supporting Figures

4.1 Cartwheel migrator binding geometry difference on short and long track

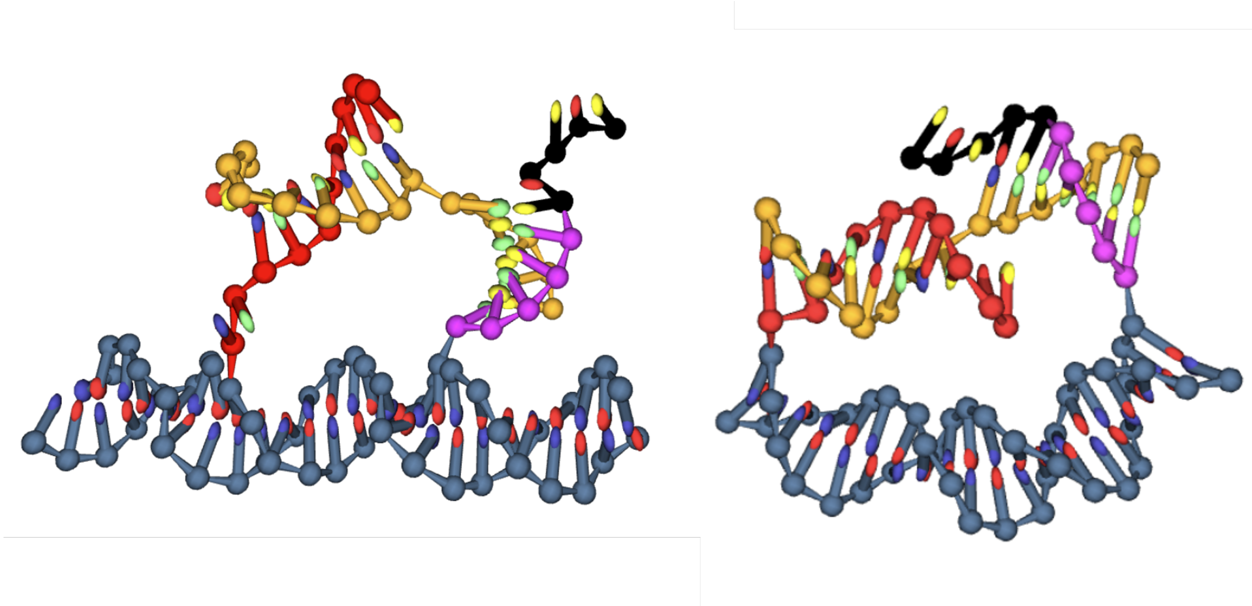

SFigure 4: The difference in binding geometry of the 15nt cartwheel migrator on 10bp track(left) and 20bp track(right). The black strand represents the foothold strand that should invade the migrator. The short track causes the migrator to bend, which reduces the strand invasion's effectiveness.

4.2 Bending angle distribution of different migrators

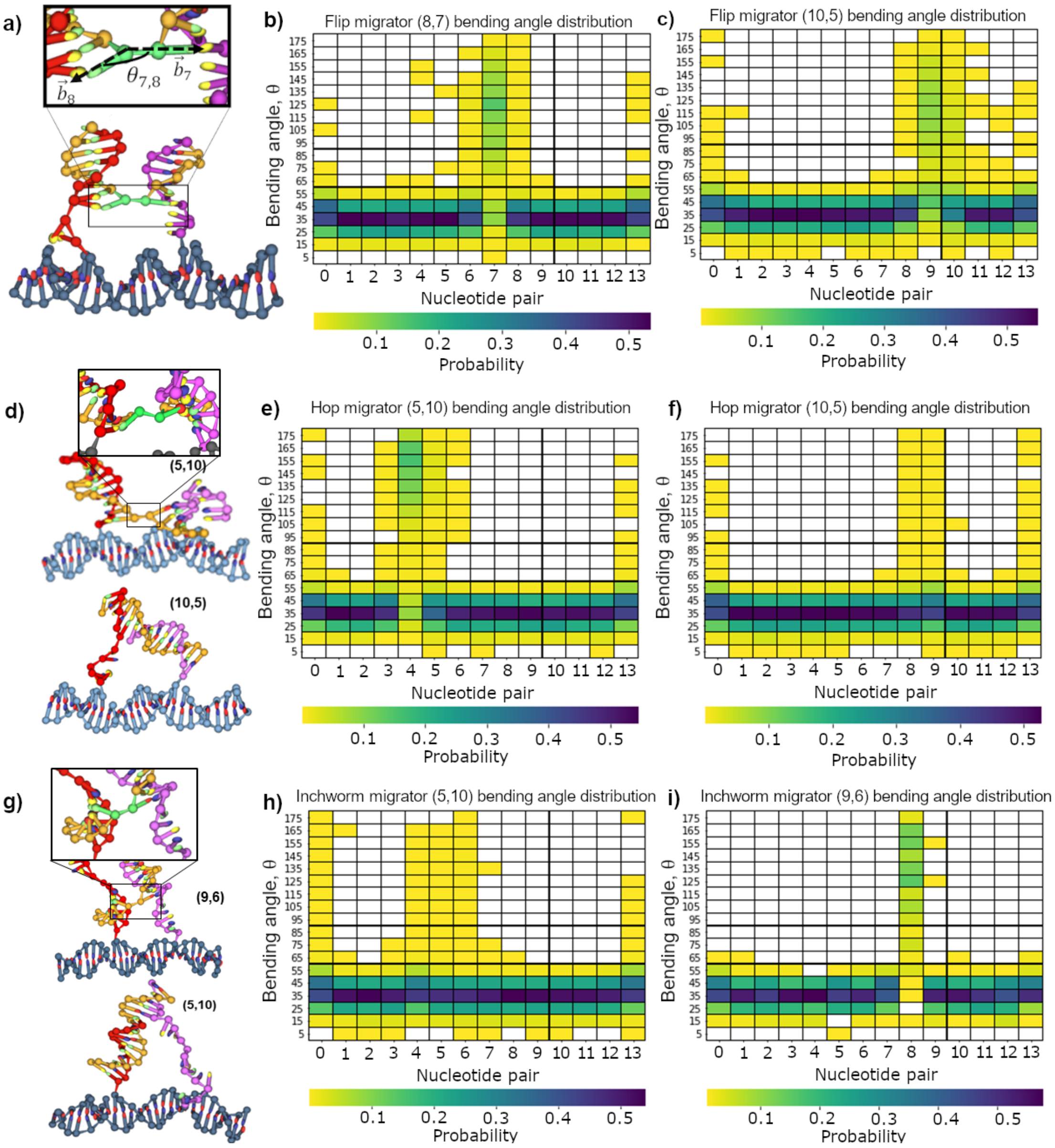

SFigure 5: The intermediate structures and the 2D histogram of migrator's bending angle in different intermediate states. **(a)** The bending angle $\theta_{i,i+1}$ is the angle between the backbone-base vectors. The backbone-base vector for the 7-th and 8-th migrator's nucleotide (highlighted in green) are shown in black arrows. **(b)-(c)** The bending angle distribution of a flipping migrator in the (8,7) and (10,5) state. **(d)** The typical configuration of a hopping migrator in (5,10) and (10,5) state. **(e)-(f)** The bending angle distribution of a hopping migrator in the (5,10) and (10,5) state. **(g)** The typical configuration of a downhill inchworm migrator in the (9,6) and the (5,10) state. **(h)-(i)** The bending angle distribution of a downhill inchworm migrator.

4.3 Free energy landscape of a flipping migrator

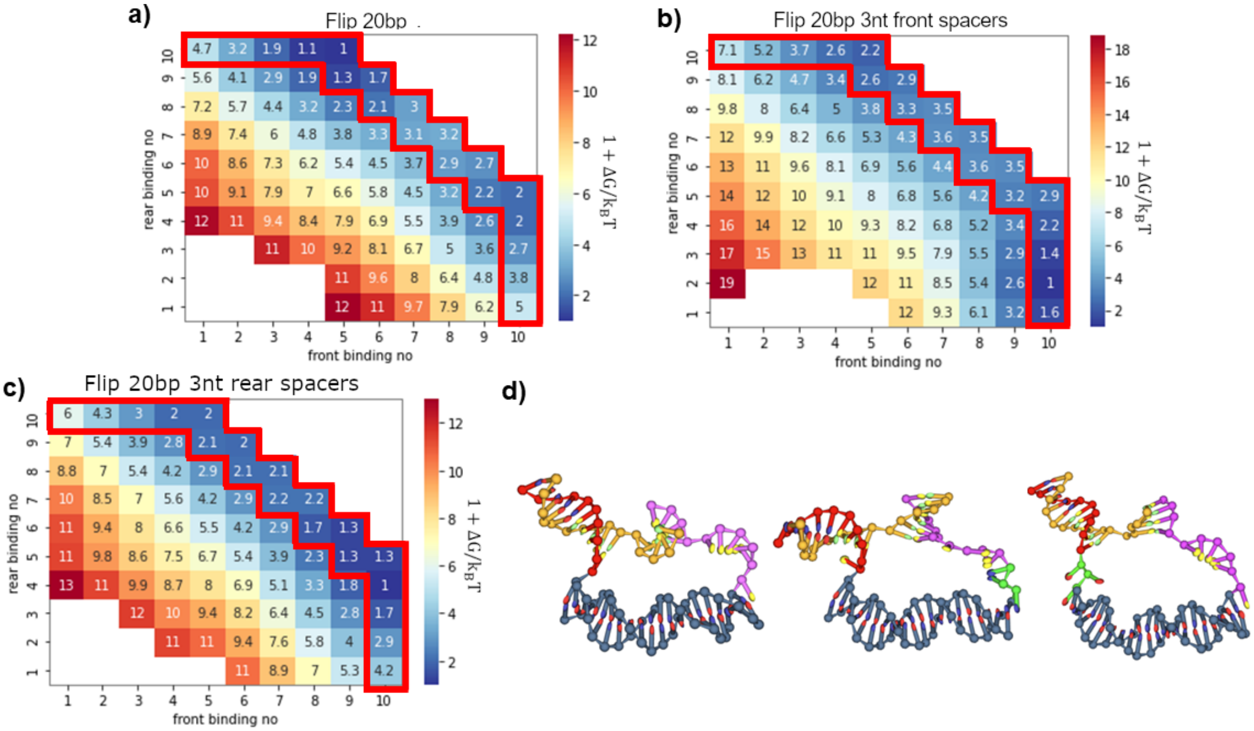

SFigure 6: 2D free energy landscapes of the flip migrator. **(a-c)** The free energy landscape of 15nt long migrator on a 20bp track, 20bp with 3nt front spacers track, and 20bp with 3nt rear spacers track. **(d)** The typical binding configuration of a flip migrator on a 20bp track(left), 20bp with 3nt front spacers track(middle) and 20bp with 3nt rear spacers track(right).

4.4 Free energy landscape of a cartwheel migrator

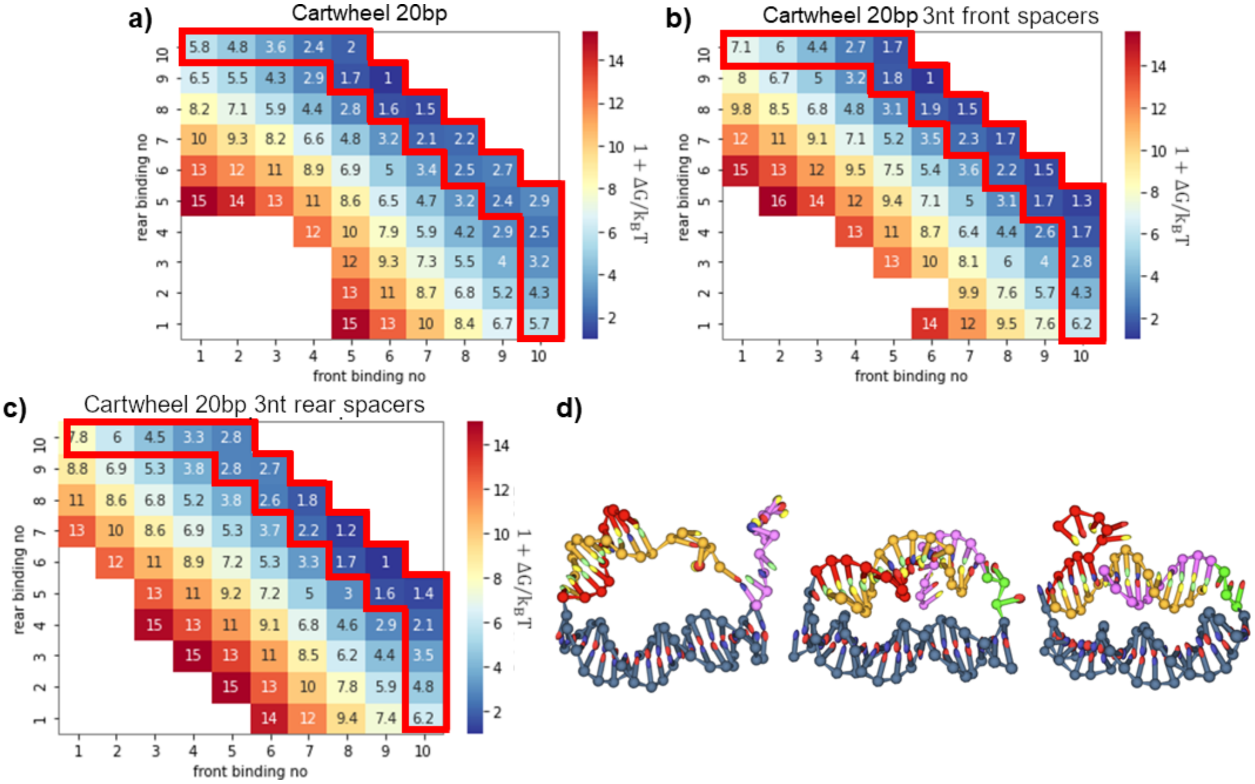

SFigure 7: 2D free energy landscapes of a cartwheeling migrator. **(a-c)** The free energy landscape of 15nt long migrator on 20bp track, 20bp with 3nt front spacers track, and 20bp with 3nt rear spacers track. **(d)** The typical binding configuration of a cartwheeling migrator on a 20bp track(left), 20bp with 3nt front spacers track(middle) and 20bp with 3nt rear spacers track(right).

4.5 Free energy landscape of a hopping migrator

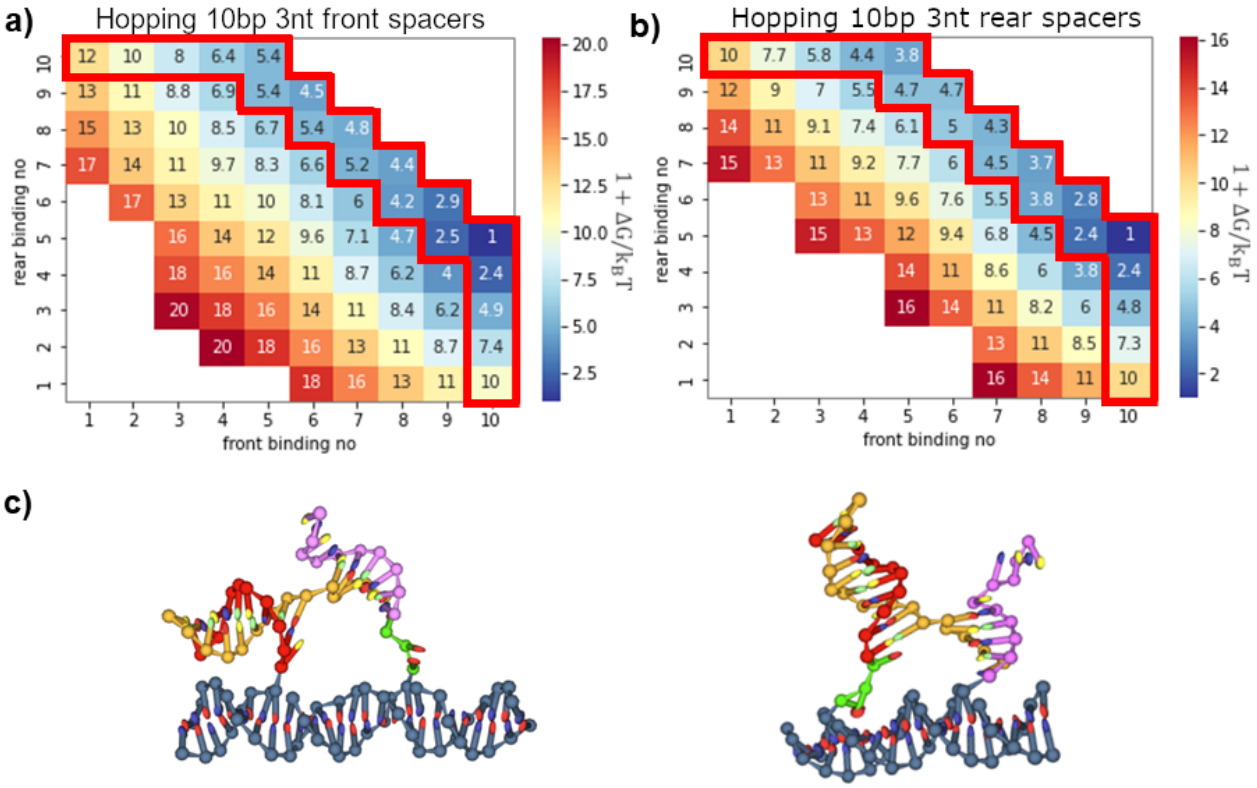

	1	2	3	4	5	6	7	8	9	10
10	12	10	8	6.4	5.4					
9	13	11	8.8	6.9	5.4	4.5				
8	15	13	10	8.5	6.7	5.4	4.8			
7	17	14	11	9.7	8.3	6.6	5.2	4.4		
6		17	13	11	10	8.1	6	4.2	2.9	
5			16	14	12	9.6	7.1	4.7	2.5	1
4			18	16	14	11	8.7	6.2	4	2.4
3			20	18	16	14	11	8.4	6.2	4.9
2				20	18	16	13	11	8.7	7.4
1						18	16	13	11	10

	1	2	3	4	5	6	7	8	9	10
10	10	7.7	5.8	4.4	3.8					
9	12	9	7	5.5	4.7	4.7				
8	14	11	9.1	7.4	6.1	5	4.3			
7	15	13	11	9.2	7.7	6	4.5	3.7		
6			13	11	9.6	7.6	5.5	3.8	2.8	
5			15	13	12	9.4	6.8	4.5	2.4	1
4					14	11	8.6	6	3.8	2.4
3					16	14	11	8.2	6	4.8
2							13	11	8.5	7.3
1							16	14	11	10

SFigure 8: 2D free energy landscapes of the hopping migrator. **(a-b)** The free energy landscape of 15nt long migrator on a 10bp with 3nt front spacers track, and 10bp with 3nt rear spacers track. **(c)** The typical binding configuration of a hopping migrator on a 10bp with 3nt front spacers track(left) and 10bp with 3nt rear spacers track(right).

4.6 Free energy landscape of a downhill inchworm migrator

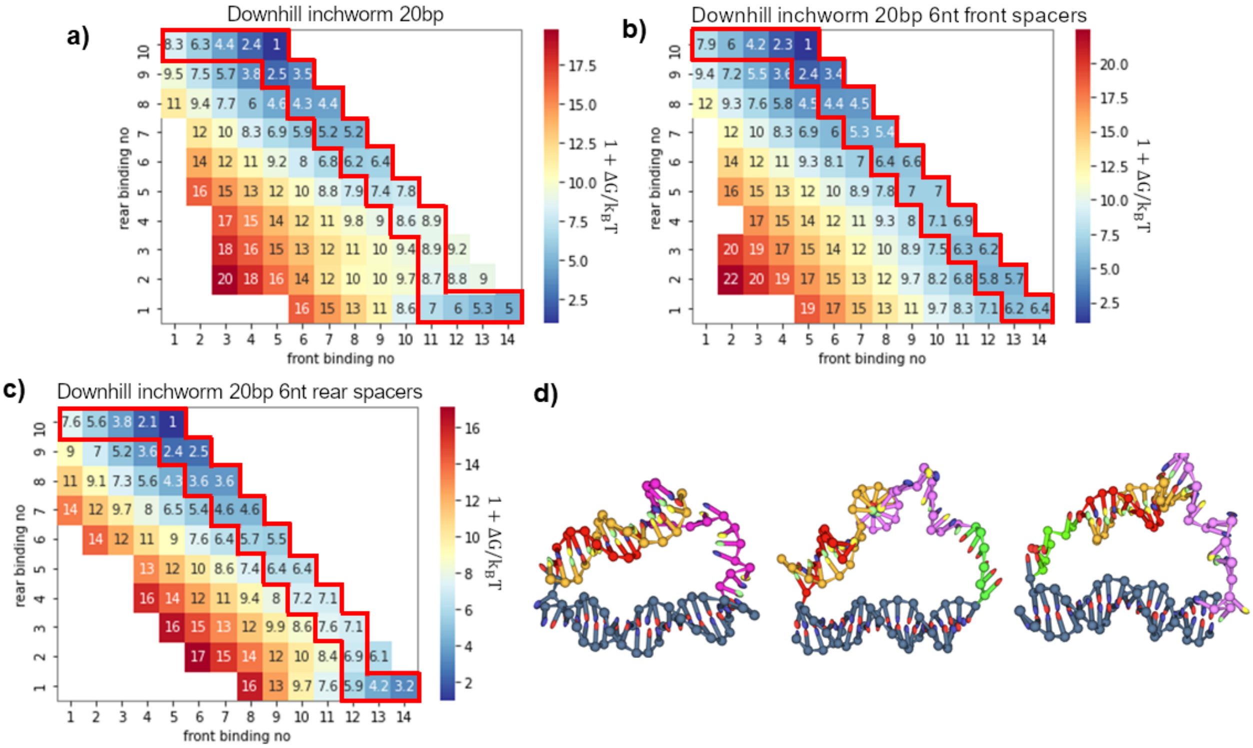

SFigure 9: 2D free energy landscapes of the downhill inchworm migrator. **(a-c)** The free energy landscape of a 15nt long migrator on a 20bp track, 20bp with 6nt front spacers track, and 20bp with 6nt rear spacers track. **(d)** The typical binding configuration of a downhill inchworm migrator on a 20bp track(left), 20bp with 6nt front spacers track(middle) and 20bp with 6nt rear spacers track(right).